



## A series of iridium complexes equipped with inert shields: Highly efficient bluish green emitters with reduced self-quenching effect in solid state

Wei He<sup>a,\*</sup>, Da-jian Zu<sup>b</sup>, De-min Liu<sup>a</sup>, Ran Cheng<sup>b</sup>

<sup>a</sup> College of Optoelectronic Science and Engineering, Huazhong University of Science and Technology, 1037 Luoyu Road, Wuhan 430074, PR China

<sup>b</sup> School of Chemistry and Chemical Engineering, Huazhong University of Science and Technology, 1037 Luoyu Road, Wuhan 430074, PR China

### ARTICLE INFO

#### Article history:

Received 12 May 2010

Received in revised form 11 August 2010

Accepted 19 August 2010

Available online 27 August 2010

#### Keywords:

Iridium complex

Bluish green

Self-quenching

Inert shield

### ABSTRACT

In this paper, we synthesize a series of cyclometalated ligands and their corresponding Ir(III) complexes using pentane-2,4-dione as the auxiliary ligand. We discuss the photophysical properties of these Ir(III) complexes in detail, including their UV–Vis absorption spectra, photoluminescence spectra in solid and liquid states, luminescence decay lifetimes, and luminescence quantum yields. The correlation between self-quenching effect and molecular structure is also investigated. It is found that these Ir(III) complexes are solid-emitting ones due to their reduced self-quenching in solid state. Theoretical calculation and experimental data reveal that the following two reasons should be responsible for the reduced self-quenching in solid state: (1) pentane-2,4-dione, phenyl, and triphenylamine moieties serve as inert shields for the excited state Ir(III) complexes; (2) the radiative decay process in these Ir(III) complexes is accelerated by the introduction of electron-donors, and thus partly immune from self-quenching caused by intermolecular action.

© 2010 Elsevier B.V. All rights reserved.

### 1. Introduction

Since the first report of phosphorescent porphyrin platinum as a highly efficient emitter in organic light emitting diodes (OLEDs), the scope and diversity of study on transition-metal complexes have continued to expand at an exponential rate due to the potential advantage of achieving a maximum internal quantum efficiency of 100% [1]. Particularly, the second- and third-row transition-metal complexes incorporating chelating chromophores, such as 2,2'-bipyridine and 2-phenyl pyridine, have attracted a great deal of study [2]. In this series, Ir(III) cores are particularly promising because of their favorable short phosphorescence lifetimes, well-suited energy levels, thermal stability, and environmental inertness. In exploring high efficiency phosphorescent emitters and moving towards materials with the required color gamut for full color displays, many efforts have been devoted to develop tricolor-emitting phosphorescent materials, and a good harvest of Ir(III) complexes covering the whole visible region has been achieved [3–7]. Unfortunately, most of the reported phosphorescent emitters based on Ir(III) complexes suffer badly from self-quenching at high concentration, leading to luminescence decrease or even absence [8,9]. The host–guest emitting system has been raised and used to overcome this disadvantage: by doping and thus isolating emitter molecules into host materials which are responsible for both

charge-carrier and energy transportation, the intense self-quenching can be avoided. However, this doped device structure at the same time complicates device fabrication procedure, leading to somewhat poor repeatability.

Recently, several research groups have reported phosphorescence OLEDs with non-doped device structures, and exciting results have been realized. For example, Burn and co-workers report a class of phosphorescent dendrimers composed of an Ir(III) core, metal-bonded phenylene dendrons, and 2-ethylhexyloxy surface groups which, however, are not sufficient enough to eliminate the interactions between emitting cores [10]. What's more, Huang and Cheng also demonstrate novel Ir(III)-based emitters for non-doped phosphorescent OLEDs, and a luminous efficiency of 34.7 cd/A with an external quantum efficiency of 10.3% is finally reported [11,12]. Those reports enlighten a practicable way of simplifying OLED fabrication procedure.

Despite their exciting device performances, such phosphorescent Ir(III)-based emitters for non-doped device structures are still rare, and the correlation between self-quenching effect and molecular structure is far from developed. Guided by above considerations, we devote our initial effort to the synthesis of Ir(III)-based emitters with reduced self-quenching effect, as well as to the correlation between self-quenching effect and molecular structure. In this paper, we synthesize a series of cyclometalated ligands (C<sup>N</sup> ligands) equipped with various moieties, and their corresponding Ir(III) complexes. The photophysical properties, including UV–Vis absorption spectra, PL spectra in solid and liquid states, luminescence decay

\* Corresponding author. Tel.: +86 27 87692130; fax: +86 27 87694034.

E-mail address: [heweilliam1005@163.com](mailto:heweilliam1005@163.com) (W. He).

lifetimes, and luminescence quantum yields, are discussed in detail. The correlation between self-quenching effect and molecular structure is also investigated.

## 2. Experimental

All starting materials, including  $I_2$ , pentane-2,4-dione (Hacac), benzene-1,2-diamine,  $IrCl_3 \cdot 3H_2O$ , benzaldehyde, 4-methoxy-benzaldehyde, 4-dimethylamino-benzaldehyde, triphenylamine, 9H-carbazole, polyvinylpyrrolidone (PVP), and bromoethane were purchased from Aldrich Chemical Co. and used without further purification unless otherwise stated. Organic solvents were carefully dried and distilled prior to use. 4-Diphenylamino-benzaldehyde and 9-ethyl-9H-carbazole-3-carbaldehyde were synthesized according to the literature procedures [13,14].

### 2.1. Synthesis of ligands

Scheme 1 shows the synthetic procedure for C<sup>N</sup> ligands and their corresponding Ir(III) complexes. 1-Benzyl-2-phenyl-1H-benzo[d]imidazole (L1), 1-(4-methoxybenzyl)-2-(4-methoxyphenyl)-1H-benzo[d]imidazole (L2), 4-(1-(4-(dimethylamino)benzyl)-1H-benzo[d]imidazol-2-yl)-N,N-dimethylaniline (L3), 4-(1-(4-(diphenylamino)benzyl)-1H-benzo[d]imidazol-2-yl)-N,N-diphenylaniline (L4), and 9-ethyl-3-(1-(9-ethyl-9H-fluoren-2-yl) methyl)-1H-benzo[d]

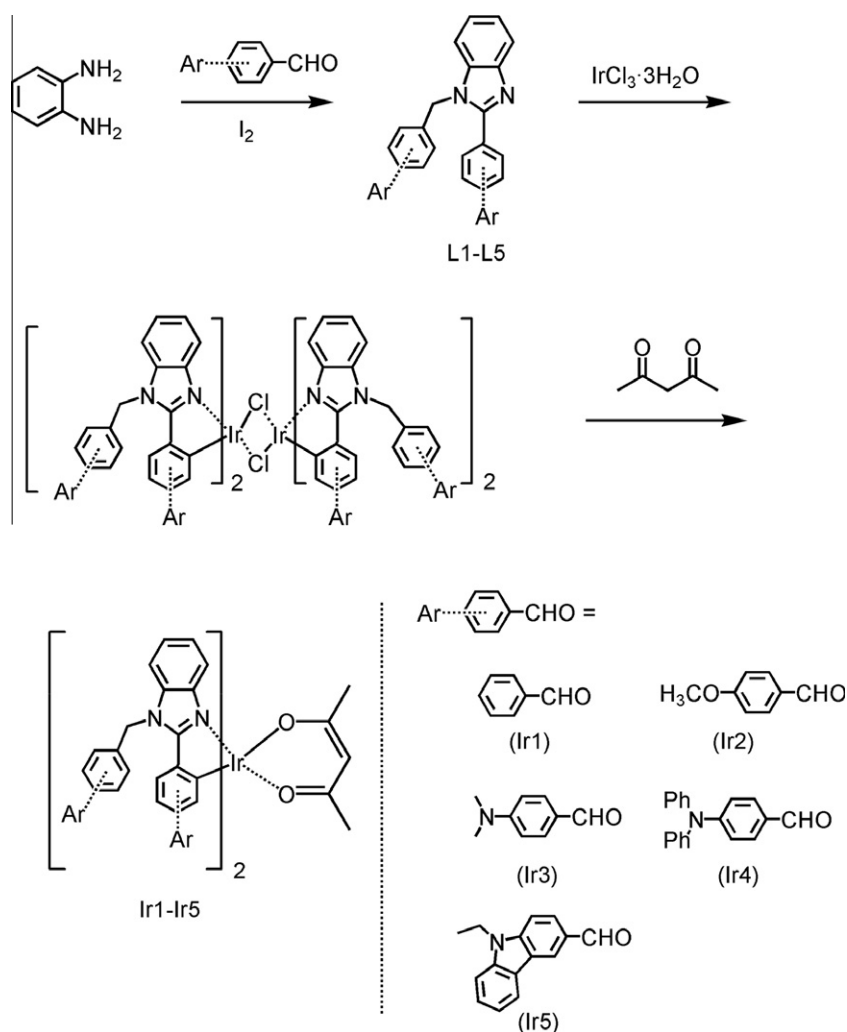
imidazol-2-yl)-9H-carbazole (L5) were synthesized according to the literature procedure [15]. A typical synthetic procedure for L1 is described as follows.

L1. The mixture of 10 mmol of 1,2-phenylenediamine, 20 mmol of benzaldehyde, 0.2 mmol of iodine, and 20 mL of THF:H<sub>2</sub>O (V:V = 1:1) was stirred for 5 h at 80 °C. After cooling, the mixture were extracted with CH<sub>2</sub>Cl<sub>2</sub> and further purified by column chromatography on silica gel to give the pure product as white powder. <sup>1</sup>H NMR (CDCl<sub>3</sub>, 300 MHz) δ [ppm]: 5.47 (s, 2H), 7.10 (d, 2H), 7.31 (m, 2H), 7.35 (m, 2H), 7.46 (m, 4H), and 7.70 (d, 2H).

L2. The synthetic procedure for L2 is similar with that of L1 except that benzaldehyde was replaced by 4-methoxy-benzaldehyde. <sup>1</sup>H NMR (CDCl<sub>3</sub>, 300 MHz) δ [ppm]: 3.76 (s, 3H), 3.84 (s, 3H), 5.39 (s, 2H), 6.85 (d, 2H), 6.96 (d, 2H), 7.04 (d, 2H), 7.23 (m, 2H), 7.27 (d, 2H), and 7.62 (d, 2H).

L3. The synthetic procedure for L3 is similar with that of L1 except that benzaldehyde was replaced by 4-dimethylamino-benzaldehyde. <sup>1</sup>H NMR (CDCl<sub>3</sub>, 300 MHz) δ [ppm]: 2.93 (s, 6H), 3.01 (s, 6H), 5.37 (s, 2H), 6.68 (m, 2H), 6.73 (d, 2H), 7.02 (d, 2H), 7.20 (d, 2H), 7.64 (d, 2H), and 7.83 (d, 2H).

L4. The synthetic procedure for L4 is similar with that of L1 except that benzaldehyde was replaced by 4-diphenylamino-benzaldehyde. <sup>1</sup>H NMR (CDCl<sub>3</sub>, 300 MHz) δ [ppm]: 5.43 (s, 2H), 6.98 (d, 6H), 7.05 (d, 2H), 7.08 (m, 4H), 7.12 (m, 8H), 7.15 (m, 3H), 7.23 (m, 3H), and 7.31 (d, 6H).



Scheme 1. A synthetic procedure for C<sup>N</sup> ligands and their corresponding Ir(III) complexes.

L5. The synthetic procedure for L5 is similar with that of L1 except that benzaldehyde was replaced by 9-ethyl-9H-carbazole-3-carbaldehyde.  $^1\text{H}$  NMR ( $\text{CDCl}_3$ , 300 MHz)  $\delta$  [ppm]: 1.41 (d, 6H), 4.32 (d, 4H), 5.73 (s, 2H), 7.17 (m, 5H), 7.39 (d, 8H), and 7.93 (d, 5H).

## 2.2. Synthesis of Ir(III) complexes

A typical synthetic procedure for the Ir(III) complexes of Ir1–Ir5 is described as follows [16]. Of  $\text{IrCl}_3 \cdot 3\text{H}_2\text{O}$  (0.68 mmol) and 1.8 mmol of C^N ligand (L1, L2, L3, L4, or L5) was added into the mixed solvent of 2-ethoxyethanol (15 mL) and water (5 mL). The mixture was refluxed for 48 h under  $\text{N}_2$  atmosphere. After cooling, a small quantity of cold water was added to give solid product. The dried product of chloro-bridged dimer was mixed with 2.1 mmol of anhydrous sodium carbonate, 25 mL of 2-ethoxyethanol, and 2.1 mmol of Hacac. The mixture was refluxed for 16 h. After cooling, water as added to give colored product. The crude product was further purified on silica gel to give pure samples.

Ir1.  $^1\text{H}$  NMR ( $\text{CDCl}_3$ , 300 MHz)  $\delta$  [ppm]: 2.10 (d, 6H), 3.49 (m, 1H), 5.45 (s, 4H), 6.84 (d, 4H), 6.96 (m, 4H), 7.06 (m, 2H), 7.10 (m, 8H), and 7.36 (d, 4H). *Anal. Calc.* for  $\text{C}_{45}\text{H}_{37}\text{N}_4\text{O}_2\text{Ir}$ : C, 62.99; H, 4.34; N, 6.53. *Found*: C, 63.13; H, 4.72; N, 6.31%.

Ir2.  $^1\text{H}$  NMR ( $\text{CDCl}_3$ , 300 MHz)  $\delta$  [ppm]: 2.06 (d, 6H), 3.50 (m, 1H), 3.70 (s, 6H), 3.70 (s, 6H), 5.47 (s, 4H), 6.62 (d, 4H), 6.76 (d, 4H), 6.97 (d, 2H), 7.05 (m, 4H), 7.11 (d, 4H), and 7.36 (d, 4H). *Anal. Calc.* for  $\text{C}_{49}\text{H}_{45}\text{N}_4\text{O}_6\text{Ir}$ : C, 60.17; H, 4.64; N, 5.72. *Found*: C, 59.84; H, 4.91; N, 6.01%.

Ir3.  $^1\text{H}$  NMR ( $\text{CDCl}_3$ , 300 MHz)  $\delta$  [ppm]: 2.12 (d, 6H), 3.04 (s, 12H), 3.12 (s, 12H), 3.55 (m, 1H), 5.46 (s, 4H), 6.46 (m, 4H), 6.89 (d, 4H), 6.94 (d, 2H), 7.24 (d, 4H), 7.80 (d, 4H), and 7.99 (d, 4H). *Anal. Calc.* for  $\text{C}_{53}\text{H}_{57}\text{N}_8\text{O}_2\text{Ir}$ : C, 61.78; H, 5.58; N, 10.88. *Found*: C, 61.94; H, 5.97; N, 10.59%.

Ir4.  $^1\text{H}$  NMR ( $\text{CDCl}_3$ , 300 MHz)  $\delta$  [ppm]: 2.07 (d, 6H), 3.55 (m, 1H), 5.55 (s, 4H), 6.85 (d, 6H), 6.85 (d, 6H), 6.90 (m, 4H), 7.04 (m, 16H), 7.18 (m, 8H), 7.20 (m, 10H), and 7.20 (d, 12H). *Anal. Calc.* for  $\text{C}_{93}\text{H}_{73}\text{N}_8\text{O}_2\text{Ir}$ : C, 73.16; H, 4.82; N, 7.34. *Found*: C, 72.98; H, 5.11; N, 7.54%.

Ir5.  $^1\text{H}$  NMR ( $\text{CDCl}_3$ , 300 MHz)  $\delta$  [ppm]: 1.46 (d, 12H), 2.09 (d, 6H), 3.52 (m, 1H), 4.03 (d, 8H), 5.68 (s, 4H), 6.86 (m, 10H), 7.362 (d, 14H), and 7.64 (d, 10H). *Anal. Calc.* for  $\text{C}_{77}\text{H}_{65}\text{N}_8\text{O}_2\text{Ir}$ : C, 69.71; H, 4.94; N, 8.45. *Found*: C, 69.53; H, 5.07; N, 8.67%.

## 2.3. Methods and measurements

$^1\text{H}$  NMR spectra were recorded on a Bruker AVANCE 300 MHz spectrometer. Element analyses were performed using a Vario Element Analyzer. UV–Vis absorption spectra were obtained with a Shimadzu UV-3101PC spectrophotometer. Solid state photoluminescence (PL) spectra of the five Ir(III) complexes were measured in powders with a Hitachi F-4500 fluorescence spectrophotometer. Solid state PL quantum yields were measured in films using the Hitachi F-4500 fluorescence spectrophotometer equipped with an integrating sphere. All films for PL record were obtained by evaporating their corresponding  $\text{CH}_2\text{Cl}_2$  solutions on quartz substrates. PL quantum yields in solutions were measured with the Hitachi F-4500 fluorescence spectrophotometer according to the literature procedure [13]. PL decay data were measured by a quanta ray DCR-3 pulsed Nd:YAG laser system in solution excited by laser pulse at wavelength 355 nm. The Nd:YAG laser possesses a line width of  $1.0\text{ cm}^{-1}$ , pulse duration of 10 ns and repetition frequency of 10 Hz. A Rhodamine 6G dye pumped by the same Nd:YAG laser was used as the frequency-selective excitation source. Time-dependent density functional theory (TD-DFT) calculations were performed on Ir1 and Ir4 with GAMESS at RB3PW91/SBKJC level.

Their initial structures were optimized by MOPAC 2009 with PM6 Hamilton.

## 3. Results and discussion

### 3.1. Absorption of Ir(III) complexes

As mentioned above, we introduce various moieties into C^N ligands to investigate the correlation between self-quenching effect and molecular structure. Here, we firstly inspect their effect on UV–Vis absorption of the corresponding Ir(III) complexes. Fig. 1 shows the UV–Vis absorption spectra of the five Ir(III) complexes, Ir1–Ir5, in  $\text{CH}_2\text{Cl}_2$  solutions with a concentration of  $1 \times 10^{-5}\text{ mol/L}$ . It is observed that each absorption spectrum is composed of an intense multiple absorption band in ultraviolet region from 220 to 340 nm and a weak absorption band ranging from 340 to 520 nm. The high energy absorption bands are assigned to spin-allowed  $\pi\text{--}\pi^*$  transitions of the C^N ligands according to the literature reports [16,17]. As for the low energy ones, they are experimentally assigned to the absorption of singlet and triplet metal-to-ligand-charge-transfer (MLCT) transitions. For example, the broad absorption of Ir1 ranging from 340 to 514 nm is composed of  $^1\text{MLCT}$  and  $^3\text{MLCT}$  transitions, and their corresponding absorption intensity values are found to be similar. Above phenomenon suggests that the  $^3\text{MLCT}$  transition is strongly allowed by the effective mixing of singlet-triplet with higher lying spin-allowed transitions on the C^N ligand, and this mixing is facilitated by the strong spin-orbit coupling of iridium center [16,17]. Similarly, the other four complexes also demonstrate  $^1\text{MLCT}$  and  $^3\text{MLCT}$  absorption bands. In addition, the optical absorption edges ( $\lambda_{\text{edg}}$ ) of the five Ir(III) complexes occupy a narrow region of 500–530 nm as shown by the inset of Fig. 1, which may be caused by their similar C^N ligands. Thus, it is expected that various moieties incorporated by inert chain of methylene exhibit no obvious effects on the onset electronic transition of these Ir(III) complexes.

### 3.2. Theoretical calculations on Ir(III) complexes

In order to get a further understanding on the electronic nature of these Ir(III) complexes, we perform a DFT/TD-DFT calculation, which has been proved to be a powerful tool to investigate the electronic properties of transition-metal complexes, on two typical Ir(III) complexes of Ir1 and Ir4 at B3PW91/SBKJC level [18]. The selected geometric parameters are listed in Table 1, along with the graphic presentations of frontier molecular orbitals (MOs) for Ir1 and Ir4 shown in Fig. 2A and B. The calculated structural param-

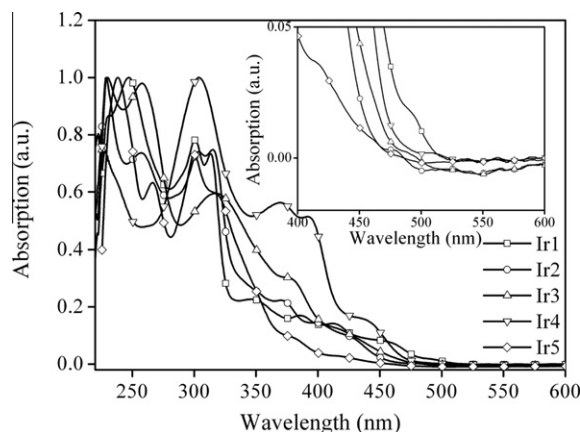
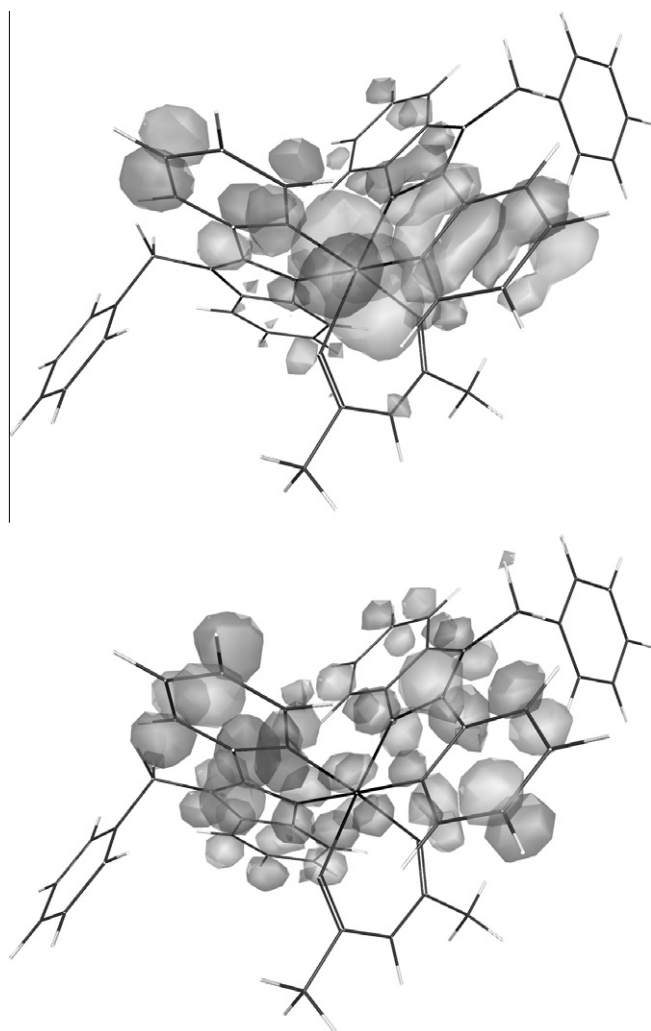


Fig. 1. UV–Vis absorption spectra of the five Ir(III) complexes in  $\text{CH}_2\text{Cl}_2$  solutions with a concentration of  $1 \times 10^{-5}\text{ mol/L}$ .

**Table 1**  
Selected geometric parameters of Ir1 and Ir4 calculated at RB3PW91/SBKJC level.

Ir1				Ir4			
Bond length	(Å)	Bond angle	(°)	Bond length	(Å)	Bond angle	(°)
Ir–N1	2.035	N1–Ir–C1	82.3	Ir–N1	2.034	N1–Ir–C1	82.5
Ir–C1	1.929	N2–Ir–C2	81.8	Ir–C1	1.933	N2–Ir–C2	82.1
Ir–N2	2.063	O1–Ir–O2	91.2	Ir–N2	2.057	O1–Ir–O2	91.5
Ir–C2	1.968	N1–Ir–O1	176.0	Ir–C2	1.976	N1–Ir–O1	87.3
Ir–O1	2.129	N1–Ir–O2	88.6	Ir–O1	2.179	N1–Ir–O2	175.3
Ir–O2	2.182	N2–Ir–O1	85.7	Ir–O2	2.126	N2–Ir–O1	93.5
		N2–Ir–O2	93.6			N2–Ir–O2	86.3



**Fig. 2A.** HOMO (up) and LUMO (down) of Ir1 calculated at RB3PW91/SBKJC level.

ters fit well with those obtained from single crystals, confirming the correctness of these optimized structures [16,19]. Not surprisingly, the Ir(III) ion occupies the center of a distorted octahedral environment, which is consistent with literature reports [16,19].

The calculated percentage composition of frontier molecular orbitals for Ir1 and Ir4, as well as their singlet ( $S_1$ ) and triplet ( $T_1$ ) excitation energy values, are shown in Tables 2A and 2B. As for Ir1, the highest occupied molecular orbital (HOMO) of Ir-POP (MO 133) is found to have a dominant character of Ir, admixed with large contributions from L1 ligand, but the contribution from acac is slim. The cases for HOMO–1 (MO 132), HOMO–2 (MO 131) are similar with that for HOMO. As for HOMO–3 (MO 130) and

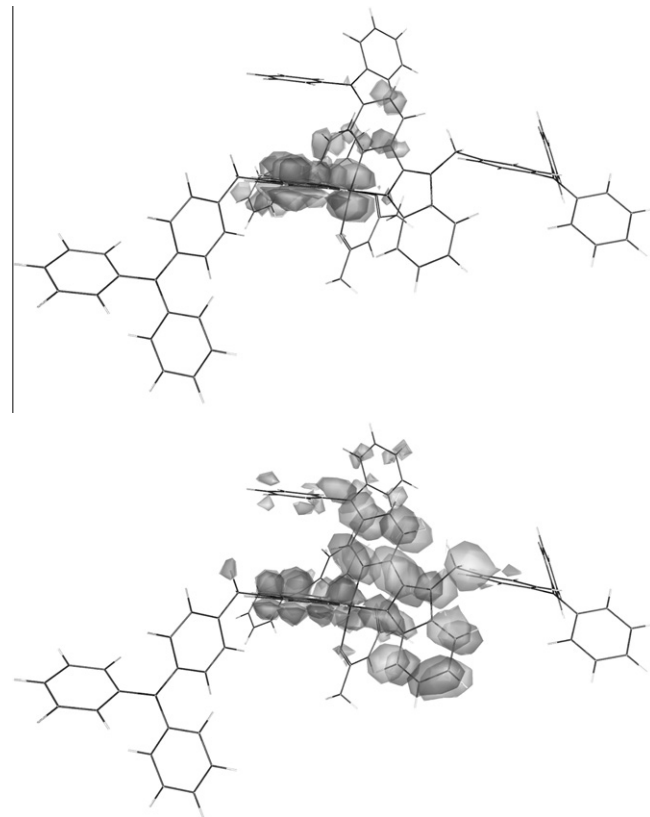


**Fig. 2B.** HOMO (up) and LUMO (down) of Ir4 calculated at RB3PW91/SBKJC level.

HOMO–4 (MO 129), however, the contributions from Ir center decrease largely. Correspondingly, the contributions from acac to MO 130 and MO 129 increase. On the other hand, the lowest unoccupied molecular orbital (LUMO, MO 134) and LUMO+1 (MO 135) are essentially  $\pi^*$  orbitals from L1, along with the minor contributions from acac and Ir center.

The singlet and triplet electronic transitions involving frontier molecular orbitals (MO) of 129–136 are thus assigned to be MLCT ones, admixed with large contributions from innerligand charge-transfer (ILCT) and ligand-to-ligand-charge-transfer (LLCT). The singlet onset electronic transition of  $S_0 \rightarrow S_1$  is essentially the electronic transition from MO 133 to 134 with transition energy of 431 nm. While, the triplet onset electronic transition of  $S_0 \rightarrow T_1$  consists of electronic transitions of MO 133 to 134 and MO133 to 135, with transition energy of 508 nm. The calculated  $S_0 \rightarrow T_1$  energy is so close to the  $\lambda_{\text{edg}}$  obtained from the absorption spectrum of Ir1. Similar case is also observed for Ir4 as shown in Table 2B. The occupied frontier MOs have a dominant Ir character, while the unoccupied MOs are essentially  $\pi^*$  orbitals from L4. The calculated  $S_0 \rightarrow T_1$  energy of Ir4 is also close to the  $\lambda_{\text{edg}}$  obtained from

**Table 2A**  
Calculated percentage composition of frontier MOs for Ir1, as well as the first five singlet and triplet excitation energy values.

MO&transition	Energy	Character	Contribution (%)		
			Ir	C^N ligand	acac
136(V)	−0.678 eV	acac&L1	5.8	46.7	47.6
135(V)	−1.233 eV	L1	4.6	90.6	4.8
<b>134(V)</b>	−1.276 eV	L1	2.0	95.7	2.3
<b>133(O)</b>	−4.865 eV	L1&Ir	39.6	47.4	13.0
132(O)	−5.050 eV	L1&Ir	41.0	44.7	14.3
131(O)	−5.412 eV	Ir&L1	46.2	42.0	11.9
130(O)	−5.731 eV	L1&acac	2.5	58.5	39.0
129(O)	−6.076 eV	L1&acac	9.2	66.9	23.9
S <sub>0</sub> → S <sub>1</sub>	431 nm	(IL&ML)CT	133 → 134(86.1)/133 → 135(10.3)		
S <sub>0</sub> → S <sub>2</sub>	425 nm	(IL&ML)CT	133 → 135(85.9)/133 → 134(9.8)		
S <sub>0</sub> → S <sub>3</sub>	402 nm	(IL&ML)CT	132 → 134(74.3)/132 → 135(21.7)		
S <sub>0</sub> → S <sub>4</sub>	396 nm	(IL&ML)CT	132 → 135(71.2)/132 → 134(19.5)		
S <sub>0</sub> → S <sub>5</sub>	368 nm	(IL&ML&LL)CT	133 → 136(94.7)		
S <sub>0</sub> → T <sub>1</sub>	508 nm	(IL&ML&LL)CT	133 → 134(41.7)/133 → 135(38.3)/130 → 135(5.4)		
S <sub>0</sub> → T <sub>2</sub>	496 nm	(IL&ML&LL)CT	133 → 135(25.3)/132 → 134(19.5)/133 → 134(18.2)/132 → 135(9.5)/130 → 134(8.3)		
S <sub>0</sub> → T <sub>3</sub>	443 nm	(IL&ML)CT	132 → 134(47.9)/132 → 135(18.4)/133 → 134(9.2)/131 → 135(8.4)/133 → 135(6.9)		
S <sub>0</sub> → T <sub>4</sub>	439 nm	(IL&ML)CT	132 → 135(41.3)/133 → 134(18.1)/131 → 134(13.1)/133 → 135(12.7)		
S <sub>0</sub> → T <sub>5</sub>	425 nm	(IL&ML&LL)CT	132 → 136(41.7)/130 → 136(23.1)/131 → 136(9.7)/129 → 136(7.3)/133 → 136(4.6)		

**Table 2B**  
Calculated percentage composition of frontier MOs for Ir4, as well as the first five singlet and triplet excitation energy values.

MO&transition	Energy	Character	Contribution (%)		
			Ir	C^N ligand	acac
259(V)	−1.165 eV	L4	3.3	92.7	3.3
<b>258(V)</b>	−1.227 eV	L4	2.1	95.4	2.5
<b>257(O)</b>	−4.653 eV	L4&Ir	14.1	80.8	5.1
256(O)	−4.759 eV	L4	9.5	89.1	1.4
255(O)	−5.010 eV	L4&Ir	29.9	58.0	12.1
254(O)	−5.099 eV	L4&Ir	27.5	59.4	13.1
S <sub>0</sub> → S <sub>1</sub>	433 nm	(IL&ML)CT	257 → 258(84.2)&254 → 258(8.0)		
S <sub>0</sub> → S <sub>2</sub>	426 nm	(IL&ML)CT	257 → 259(81.4) & 255 → 259(7.0)		
S <sub>0</sub> → S <sub>3</sub>	411 nm	(IL&ML)CT	256 → 258(75.1) & 255 → 258(10.2)		
S <sub>0</sub> → S <sub>4</sub>	406 nm	(IL&ML)CT	256 → 259(75.4) & 255 → 259(18.2)		
S <sub>0</sub> → S <sub>5</sub>	391 nm	(IL&ML)CT	255 → 258(69.7) & 256 → 258(10.5) & 254 → 258(9.8)		
S <sub>0</sub> → T <sub>1</sub>	532 nm	(IL&ML)CT	257 → 259(59.0) & 257 → 258(22.6) & 256 → 259(4.9)		
S <sub>0</sub> → T <sub>2</sub>	527 nm	(IL&ML)CT	256 → 258(61.9) & 257 → 259(9.6) & 256 → 259(7.7) & 257 → 258(5.8)		
S <sub>0</sub> → T <sub>3</sub>	446 nm	(IL&ML)CT	257 → 258(45.7) & 255 → 258(13.2) & 257 → 259(12.0) & 254 → 258(9.0) & 256 → 258(7.2)		
S <sub>0</sub> → T <sub>4</sub>	434 nm	(IL&ML)CT	256 → 259(34.1) & 254 → 259(24.7) & 255 → 259(16.3) & 254 → 258(7.8) & 256 → 258(5.0)		
S <sub>0</sub> → T <sub>5</sub>	429 nm	(IL&ML)CT	255 → 259(35.6) & 255 → 258(26.9) & 254 → 259(9.8) & 256 → 259(3.8)		

the absorption spectrum of Ir4, confirming that the low energy region of Ir1 and Ir4 absorption spectrum is composed of both singlet and triplet charge-transfer transitions as we expected.

It is also observed that the contributions from acac to frontier MOs, including both occupied and unoccupied ones, are slim. What's more, phenyl and triphenylamine moieties incorporated by the inert chain of methylene give no contribution to frontier MOs as shown in Fig. 2A and B. It is thus expected that the moieties of acac, phenyl, and triphenylamine should be isolated from photon absorption and emitting processes. Consequently, above mentioned moieties may serve as inert shields for excited state Ir(III) complexes, and then suppress the phosphorescence self-quenching caused by intermolecular interaction.

### 3.3. PL properties and photophysical parameters of Ir(III) complexes

Fig. 3 shows the PL spectra of the five Ir(III) complexes, Ir1–Ir5, in CH<sub>2</sub>Cl<sub>2</sub> solutions with a concentration of  $1 \times 10^{-5}$  mol/L. Their photophysical parameters, including  $\lambda_{\text{edg}}$ , emission peaks ( $\lambda_{\text{em}}$ ), luminescence decay lifetimes ( $\tau$ ), PL quantum yields ( $\phi$ ), radiative and non-radiative constants ( $K_r$  and  $K_{nr}$ ), are summarized in Table 3. Given their similar optical absorption edges above mentioned, it is reasonable to see that their emission peaks are similar with each

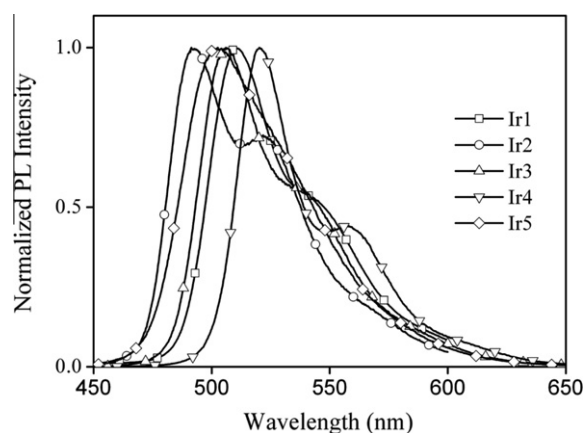


**Fig. 3.** PL spectra of the five Ir(III) complexes in CH<sub>2</sub>Cl<sub>2</sub> solutions with a concentration of  $1 \times 10^{-5}$  mol/L.

other. Their main emission peaks occupy a narrow region of 490–520 nm. As for Ir1, for example, the emission consists of a main peak of 511 nm and a shoulder peak of 544 nm. The Stokes shift

**Table 3**  
Summarized photophysical parameters of the five Ir(III) complexes.

Complex	$\lambda_{\text{edg}}$ (nm)	$\lambda_{\text{em}}$ (nm)	$\tau$ (ns)	$\Phi$ (liquid)	$\Phi$ (solid)	$K_r$ ( $\times 10^6 \text{ s}^{-1}$ )	$K_{\text{nr}}$ ( $\times 10^6 \text{ s}^{-1}$ )
Ir1	514	511, 544	97.5	0.36	0.28	3.7	6.5
Ir2	502	491, 519	84.2	0.59	0.50	7.0	7.9
Ir3	520	510, 542	50.1	0.50	0.46	10.2	9.7
Ir4	530	520, 557	96.5	0.71	0.67	7.4	3.0
Ir5	500	502	48.8	0.46	0.42	12.1	13.7

values between  $\lambda_{\text{edg}}$  and  $\lambda_{\text{em}}$  are slim, and there are even overlap between the absorption edges and emission spectra, suggesting that the emissive states of the five Ir(III) complexes are highly restricted ones and suffer from no serious geometric distortion.

The PL quantum yields are determined in  $\text{CH}_2\text{Cl}_2$  solutions with quinine sulfate in 1.0 M sulfuric acid ( $\Phi_r = 0.546$ ) as the reference standard according a literature procedure [13]. Sample and standard solutions are degassed with no fewer than four freeze-pump-thaw cycles. Quantum yield ( $\Phi$ ) is determined according to the following expression:

$$\Phi_s = \Phi_r(B_r/B_s)(n_s/n_r)^2(D_s/D_r) \quad (1)$$

where the subscripts  $s$  and  $r$  refer to sample and reference standard solution, respectively,  $n$  is refractive index of the solvent,  $D$  is the integrated intensity, and  $\Phi$  is luminescence quantum yield. The quantity  $B$  is calculated by  $B = 1 - 10^{-AL}$ , where  $A$  is the absorption coefficient at the excitation wavelength and  $L$  is the optical length. The PL quantum yields of the five Ir(III) complexes shown in Table 3 confirm that they are all efficient emitters, and we attribute the causation of these high PL quantum yields to the strong and efficient spin-orbit coupling in Ir(III) complexes.

Even in dilute solutions, where the self-quenching effect is largely and effectively reduced, the five Ir(III) complexes still exhibit short-lived luminescence decay lifetimes on the scale of  $\sim 100$  ns as shown in Table 3. We thus come to a hypothesis that the instinct fast-decay processes are responsible for these short-lived emissive states. In order to confirm this hypothesis, we calculate the corresponding  $K_r$  and  $K_{\text{nr}}$  values as follows:

$$K_r = \Phi/\tau \quad (2)$$

$$K_{\text{nr}} = (1 - \Phi)/\tau \quad (3)$$

The  $K_r$  values are found to be typically two orders of magnitude bigger than literature ones, confirming the correctness of our hypothesis [16,20]. In addition, it is observed that the  $\Phi$  values of Ir2–Ir5 are obviously larger than that of Ir1, correspondingly,  $K_r$  values of Ir2–Ir5 are obviously larger than that of Ir1. Above data suggest that C<sup>N</sup> ligands with electron-donor moieties are positive on increasing the radiative decay process, and thus improve the luminescence quantum yield.

#### 3.4. Analysis on the causation of reduced self-quenching

Considering these short-lived emissive states, it is thus expected that the self-quenching caused by intermolecular interaction may be ineffective, leading to reduced self-quenching and consequently solid state emission from the five Ir(III) complexes. The solid emission spectra of the five Ir(III) complexes shown in Fig. 4 confirm the correctness of above expectation. The solid state emission spectra of the five Ir(III) complexes measured in powders are similar with the corresponding ones measured from dilute solutions, with very slight spectral shift. In addition, the PL quantum yields measured in solid state films suggest that all efficient PL emissions remain in solid state, and the ratio of  $\Phi(\text{solid})/\Phi(\text{liquid})$  increases with the size of inert shields, as shown in Table 3. Above data suggest that the electronic transition nature of emis-

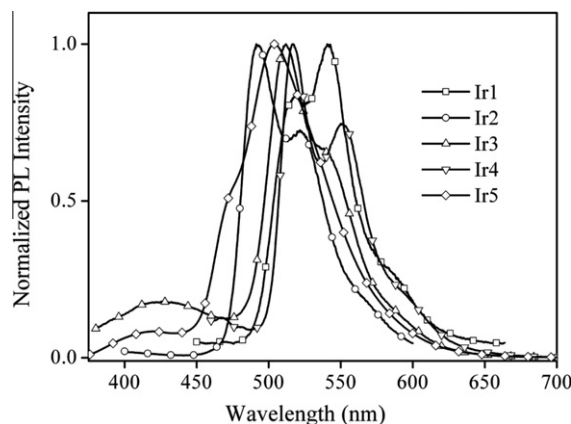


**Fig. 4.** Solid state PL spectra of the five Ir(III) complexes in powders.

sive states remains to be unaffected in solid state, and the self-quenching effect in solid state is largely and effectively reduced.

In order to further confirm the reduced self-quenching effect in solid state, we consult the PL quantum yields of doped thin films with various doping concentrations. We select the PL quantum yields of Ir4 doped in PVP as the representative data which are measured to be 0.705 for the 20 wt% doped film, 0.694 for the 40 wt% doped film, 0.687 for the 60 wt% doped film, 0.684 for the 80 wt% doped film, respectively. It is observed that the PL quantum yield changes slightly from 0.705 for a light dopant concentration of 20 wt% to 0.684 for a heavy dopant concentration of 80%, further confirming the reduced self-quenching effect in solid state.

Based on above analysis and data, we attribute the reduced self-quenching to the following two reasons. (1) As mentioned above, theoretical calculation reveals that the contributions from acac, phenyl, and triphenylamine moieties to frontier MOs are slim, and they are thus isolated from excited state processes. The above mentioned moieties may serve as inert shields for excited state Ir(III) complexes during photon absorption and emitting processes, and then suppress the phosphorescence self-quenching caused by intermolecular interaction. (2) Owing to the C<sup>N</sup> ligands equipped with electron-donor moieties, the radiative decay process is instinctively fast, making the excited state somewhat invulnerable towards the phosphorescence self-quenching caused by intermolecular interaction. Above finding may be useful when designing efficient solid state emitters for non-doped phosphorescent OLEDs.

#### 4. Conclusions

In this paper, we synthesize a series of C<sup>N</sup> ligands and their corresponding Ir(III) complexes using acac as the auxiliary ligand. We discuss the photophysical properties of these Ir(III) complexes in detail, including their UV–Vis absorption spectra, PL spectra in solid and liquid states, luminescence decay lifetimes, and luminescence quantum yields. It is found that these Ir(III) complexes are solid-emitting ones due to their reduced self-quenching in solid

state. Theoretical calculation and experimental data reveal that (1) phenyl, and triphenylamine moieties incorporated by the inert chain of methylene, as well as acac, serve as inert shields for the excited state Ir(III) complexes; (2) the radiative decay process in these Ir(III) complexes is accelerated by the introduction of electron-donors, and thus partly immune from self-quenching caused by intermolecular action. Above two reasons are attributed to be responsible for the reduced self-quenching effect as mentioned, and this conclusion may be useful when designing efficient solid state emitters for non-doped phosphorescent OLEDs.

### Acknowledgments

We gratefully acknowledge the financial support by the Education Department of Hubei Province and the Program for Innovative Research Team of Huazhong University of Science and Technology.

### References

- [1] M.A. Baldo, D.F. O'Brien, Y. You, A. Shoustikov, S. Sibley, M.E. Thompson, S.R. Forrest, *Nature* 395 (1998) 151.
- [2] A. Lavie-Cambot, M. Cantuel, Y. Leydet, G. Jonusauskas, D.M. Bassani, N.D. McClenaghan, *Coord. Chem. Rev.* 252 (2008) 2572.
- [3] J.P. Duan, P.P. Sun, C.H. Cheng, *Adv. Mater.* 15 (2003) 224.
- [4] X.W. Chen, J.L. Liao, Y.M. Liang, M.O. Ahmed, H.E. Seng, S.A. Chen, *J. Am. Chem. Soc.* 125 (2003) 636.
- [5] C.F. Chang, Y.M. Cheng, Y. Chi, Y.C. Chiu, C.C. Liu, G.H. Lee, P.T. Chou, C.C. Chen, C.H. Chang, C.C. Wu, *Angew. Chem., Int. Ed.* 47 (2008) 4542.
- [6] H. Wiedenhofer, S. Schützenmeier, A. von Zelewsky, H. Yersin, *J. Phys. Chem.* 99 (1995) 13385.
- [7] J. Schmidt, H. Wiedenhofer, A. von Zelewsky, H. Yersin, *J. Phys. Chem.* 99 (1995) 226.
- [8] S. Lamansky, P. Djurovich, D. Murphy, F. Abdel-Razzaq, H.-E. Lee, C. Adachi, P.E. Burrows, S.R. Forrest, M.E. Thompson, *J. Am. Chem. Soc.* 123 (2001) 4304.
- [9] H.J. Bolink, E. Coronado, S.G. Santamarira, M. Sessolo, N. Evans, C. Klein, E. Baranoff, K. Kalyanasundaram, M. Graetzel, M.K. Nazeeruddin, *Chem. Commun.* 31 (2007) 3276.
- [10] J.P.J. Markham, I.D.W. Samuel, S.C. Lo, P.L. Burn, M. Weiter, H. Bässler, *J. Appl. Phys.* 95 (2004) 438.
- [11] Z.W. Liu, M. Guan, Z.Q. Bian, D.B. Niu, Z.L. Gong, Z.B. Li, C.H. Huang, *Adv. Funct. Mater.* 16 (2006) 1441.
- [12] J.Q. Ding, J. Gao, Y.X. Cheng, Z.Y. Xie, L.X. Wang, D.G. Ma, X.B. Jing, F.S. Wang, *Adv. Funct. Mater.* 16 (2006) 575.
- [13] L. Zhang, B. Li, B. Lei, Z. Hong, W. Li, *J. Lumin.* 128 (2008) 67.
- [14] Y. Wang, B. Li, Y. Liu, L. Zhang, Q. Zuo, L. Shi, Z. Su, *Chem. Commun.* 39 (2009) 5868.
- [15] C.X. Li, J.W. Hu, P.P. Sun, Y. Pan, C.H. Cheng, *Chinese J. Inorg. Chem.* 23 (2007) 392.
- [16] L. Zhang, B. Li, L. Shi, W. Li, *Opt. Mater.* 31 (2009) 905.
- [17] K. Zhang, Z. Chen, C. Yang, Y. Zou, S. Gong, J. Qin, Y. Cao, *J. Phys. Chem. C* 112 (2008) 3907.
- [18] L. Yang, J.K. Feng, A.M. Ren, M. Zhang, Y.G. Ma, X.D. Liu, *Eur. J. Inorg. Chem.* 10 (2005) 1867.
- [19] M.S. Eum, C.S. Chin, S.Y. Kim, C. Kim, S.K. Kang, N.H. Hur, J.H. Seo, G.Y. Kim, Y.K. Kim, *Inorg. Chem.* 47 (2008) 6289.
- [20] S. Reineke, K. Walzer, K. Leo, *Phys. Rev. B* 75 (2007) 125328-1.